Original Research Article

Efficacy of MR Imaging in Detection of Early Vertebral Metastasis Versus Radionuclide Bone Scan

Dr. Asish Mondal, Dr. R Sundara Raja Perumal
Command hospital, (Eastern command), Kolkata

*Corresponding author
Dr. R Sundara Raja Perumal
Email: rsr_peru@yahoo.co.in

Abstract: Skeletal metastases occur with many malignancies, but they are most common in carcinomas of the breast (47-85%), prostrate (54-85%), lung (32%), kidney (33-40%), and thyroid (28-60%). Most bone metastases are hematogenous in origin, although contiguous and intraspinal spread many occur. The initial seeding of metastatic deposits via hematogenous spread is typically localized in the hematopoietic (red) marrow. This location explains the predominance of metastatic bone lesions in the axial skeleton (>90% of the metastatic bone lesions).The spine is the most common site for skeletal metastases because of the abundant vascularization and red bone marrow. Intravascular dissemination to bone can occur through the normal venous system (and occasionally the arterial system) or through Batson's plexus. Vertebral metastatic lesions amount to about 39% of all skeletal metastases. The bone scan is primarily and index of osteoblastic activity and is more sensitive to abnormalities of bony cortex and less sensitive to marrow abnormalities. Magnetic Resonance imaging (MRI) has emerged as a sensitive method of detecting intramedullay metastases in vertebral bodies, which contain large marrow content. The aim of this study is to compare the efficacy of Magnetic Resonance Imaging as against Radionuclide bone scans in early detection of vertebral metastases.
Keywords: Radio nucleotide Bone scan, MRI, Early intramedullary vertebral metastasis, Skeletal metastasis.

INTRODUCTION

Bone scan is presently the method of choice in the evaluation of skeletal metastases because of its accessibility, reasonable cost & ability to show the entire skeletal system [6]. When a tumor invades bone, it produces two changes, which are seen to varying degrees with all types of metastases. The first is bone destruction and the second is reactive bone formation or repair. It is in the latter that radioisotopes are of considerable value. In new bone formation, hydroxyapatile crystals are deposited in the osteoid matrix laid down by the osteoblasts. If sufficient radioactive atoms are available for incorporation into the hydroxyapatite crystals, the new bone can be visualized by the scintillation scanning, since the bone scan is based upon the activity of reactive bone formation, it is not specific for tumor. The scan will therefore identify any lesion in which there is active new bone formation, including fracture, infection, infarction, and other processes [7]. Early or small metastatic deposits start in the bone. Marrow. These early deposits tend to be purely intramedullary lesions without cortical involvement an may not cause sufficient osteoblastic activity to be detected on bone scans [9]. The use of MRI in metastases detection has been limited due to cost, long examination times and convenience. With the advent of faster sequences, there has been a renewed interest in MRI as a screening tool for early vertebral metastases.

Various MR sequences have been used to evaluate spinal tumors [10]. Most investigators advocate a combination of T1-weighted spone-echo and T2-Weighted spin-echo sequences [11]. In recent years faster acquisitions of STIR images have gained popularity to evaluate the bone marrow [21].

Because bone marrow (including hematopoietic or "red marrow") contains a high percentage of fat, it is reliably and readily imaged with T1-weighted spin-echo techniques because the marrow fat provides a nearly homogenous, high intensity signal. Marrow infiltration by tumor replaces normal marrow fat with tissue of increased cellularity, which shows up as areas of altered signal on various MRI sequences. Tumor, because of its long T1, is easily detected as a low-intensity defect in the marrow. Lesions can often be distinguished from deposits of red marrow on T1-weighted images because they are more focal [11]. STIR suppresses the signal from fat and shows the normal vertebral bodies as low intensity. Tumor has high intensity and is easily detected against the low-

intensity surroundings [13]. MR Imaging may offer a viable alternative to bone scan for screening for early vertebral metastases leading to early institution of treatment. This will help in reducing the morbidity and mortality associated with advanced malignancies. Objective of this study is that, MR Imaging may offer a viable alternative to bone scan for screening of early vertebral metastases which will help in reducing the morbidity associated with advanced malignancies.

EXPERIMENTAL SECTION/METHODS AND MATERIAL

Patients of are all age groups, Patient with proven malignancy and laboratories findings suspicious of metastasis were included in this study. All the patients will undergo a details clinical evaluation, a skeletal survey and any other relevant investigations as per the attached proforma, prior to Magnetic Resonance Imaging and bone scan.

Patient with pacemaker, claustrophobia, pregnancy, Schmorl's nodes, benign bone islands, and hemangiomas will be excluded from the study based on their characteristic radiological findings. The MR studies that are non-diagnostic due to technical reasons, such as patient movement or poor technical quality, would also be excluded from the study. Using the acquired data, both modalities will be compared for respective efficacy. MR imaging and bone scan will be done within 15 days of each others. Total of 60 patients were studied . Patients were enrolled in the study from referrals from various departments. These studies were conducted in the department of Radiology in collaboration with Nuclear medicine department. Parameters were studied are localization of lesions at sub cortical, intramedullary and transcortical regions and The concordance and discordance of various lesions in all the visualized vertebrae.

Conventional whole-body scintigraphy will be performed 3 hours after intravenous administration of 20 mCi (740 M Bq) or Tc-99m MDP on Siemens ECAM (Hi Definition) dual head gamma camera to be used for the whole body dynamic scan and requisite static images. No specific patient preparation was required. The patients were asked to remove jewelry, belts, change, or external prostheses and braces to avoid artifacts on the scan. After being intravenously injected with the radiopharmaceutical, the patients was encouraged to during plenty of fluids and to void prior to imaging. Three hour delayed images were obtained over the entire body in the anterior and posterior positions in all patients.

MR Imaging will be performed on a 1.5 Tesla super conductive magnet using phased array spine coil. Imaging of the vertebral column in sagittal, coronal and axial planes will be performed.

MR Imaging was performed on a 1.5 Tesla super conductive magnent using phased array spine coil. STIR of the vertebral column in sagittal and coronal planes were performed. If an abnormality was detected, further targeted T1 and T2-weighted sequences were done.

Table 1: MR Imaging reports

	AXIAl		SAGITA			CORONAL		
	T1	T2	STIR	T1	T2	STIR	T1	T2
TR (ms)	525-600	4000	5000	500-550	4000	5000	500-550	4000
TE/TI (ms)	15	90	60/150	15	90	60/150	15	90
FOV (mm)	500	500	500	500	500	500	500	500
Flip Angle (Degrees)	90	180	180	90	180	180	90	180
Slice Thickness (mm)	3-5	3-5	3.5	3.5	3.5	3.5	3.5	3.5
Matrix size	173-256	173-256	173-256	173-256	173-256	173-256	173-256	173-256

TR = time of repetition TE= Time of echo TI = Time of Inversion FOV=Field of view

No specific patient preparation was necessary other than fasting for 3-4 hours prior to the examination to avoid nausea and vomiting following administration of IV gadolinium. It was also ensured that no contraindication to MRI existed such as pacemakers, implants, implanted drug infusion device, shrapnel, ferromagnetic prosthetic valves, aneurysm clips, etc. all the patients were examined in the supine position. Scout images were first obtain in axial, coronal, and sagittal planes. Thereafter, STIR sagittal and coronal images were obtained as per above mentioned parameters. If an abnormality was detected, further targeted T1 and T2- weighted sequences were done. Paramagnetic MR contrast medium. IV gadolinium was administered as per the necessity, and T1-weighted axial and sagittal and/or coronal images were obtained.

Bone scan regions were read positive using the accepted subjective criteria such as the intensity of uptake, focality, number, location and pattern of

distribution. An area was considered abnormal when its uptake of tracer was increased compared to adjacent structures. Only the regions examined by both Magnetic Resonance Imaging and scintigraphic studies were compared. MR images were read positive if a well-defined focus of low signal intensity was seen on T1-weighted images and high signal intensity on STIR or T2-weighted images. Post IV gadolinium T1-weighted images were considered positive if the lesion exhibited contrast enhancement.

The spine was divided into cervical, upper dorsal (T1-4), middle dorsal (T5-8), lower dorsal (T9-12), lumbar (L1-5), and sacral regions. In each region the reading was scored as positive or negative for metastatic involvement. The size of each lesion was measured at its greatest dimension on MR images and was categorized as small (<2 cm) or large (>2 cm). coalescent lesions were included in the large lesion group. The relationship between the lesion and the cortical bone was classified on the basis of the sagittal and coronal STIR images by determining whether the lesion was distant from (intramedullary), had contact with (subcortical), or had invaded the bony cortex (transcortical). Subsequently images were reread with bone scan and MRI side by side to ensure that concordant lesions are truly concordant. Corresponding Magnetic Resonance Imaging and bone scan interpretations were considered concordant in a region if both readings were positive or negative for metastases and discordant if the readings differed. Confirmation of findings was sought in discordant cases using correlative modalities. Subsequent progression on repeat bone scans and MRI was considered confirmatory. The presumption made was that all focal lesions on scintigrams or MR images were metastases unless proved otherwise.

RESULTS

Patients with a proven malignancy and clinical and laboratory suspicion of vertebral metastases, who were referred to the Oncology Centre , formed the subjects of this study. Thus, 60 cases of vertebral metastases were finally included, who had undergone MR Imaging and bone scan within 15 days of each other.

The 60 patients were divided in different subgroups depending on the age and sex.

1. Age Distribution

Of the 60 patients studied, the youngest patients was aged 14 months and the eldest was 71 years. Majority of the patients (30.0%) fell into the age group of 51-60 years. The second commonest age group was 41-50 years (33.3%).

Table 2: Age distribution of the study population

S. No.	Age Group (Yrs)	No. of Cases	Percentage
1.	Upto 10	2	3.3
2.	11-20	0	0
3.	21-30	1	1.7
4.	31-40	5	8.3
5.	41-50	20	33.3
6.	51-60	21	35.0
7.	61-70	8	13.4
8.	71-80	3	5.0
	Total	60	100

2. Sex Distribution

The study included 32 males and 28 Females, forming 53.3% and 46.7% respectively.

3. Case Distribution

In our study of 60 patients with vertebral metastases, the number of cases in each primary carcinoma is given in Table -3.

Table 3: Primary Carcinomas

S. No.	Primary Carcinoma	Number of cases	percentage
1.	Carcinoma Breast	19	31.7
2.	Carcinoma Prostrate	16	26.7
3.	Carcinoma Lung	9	15.0
4.	Thyroid carcinoma	5	8.3
5.	Bladder Carcinoma	3	5.0
6.	Renal Carcinoma	3	5.0
7.	Neuroblastoma	2	3.3
8.	Adenocarcinoma Colon	2	3.3
9.	Melanoma	1	1.7
	Total	60	100

The commonest was carcinoma breast with 19 cases (31.7%). The second commonest was carcinoma prostrate with 16 cases (26.7%) and the third commonest was lung carcinoma with 9 cases (15%).

4. Age Wise Distribution of Primary Carcinomas

Table 3 shows the age wise distribution of the primary carcinomas. Commonest age group for primary carcinomas was 51-60 years with 21 cases (35%) and the second commonest was 41-50 years with 20 cases (33.3%). Carcinoma breast was commonest in the age group between 41-50 years with 7 cases (36.8%). Carcinoma prostrate was commonest in the age group between 51-60 years with 7 cases (43.8%). Carcinoma lung was commonest in the age group between 41-50 years with 3 cases (33.3%).

Table 4: Age wise distribution of primary carcinomas

Primary carcinoma	Age group (years)								Total
	0-10	11-20	21-30	31-40	41-50	51-60	61-70	71-80	
Ca Breast	0	0	0	3	7	5	4	0	19
Ca Prostrate	0	0	0	0	6	7	2	1	16
Ca Lung	0	0	0	2	3	2	1	1	09
Ca Thyroid	0	0	0	0	2	2	1	0	05
Renal Ca	0	0	0	0	1	2	0	0	03
Bladder CA	0	0	0	0	0	2	0	1	03
Neuroblastoma	2	0	0	0	0	0	0	0	02
Adenoca Colon	0	0	0	0	1	1	0	0	02
Melanoma	0	0	1	0	0	0	0	0	01
Total	2	0	1	5	20	21	8	3	60

5. Bone Scan Readings as Per Region

The spine was divided into cervical, upper thoracic (T1-6), lower thoracic (T7-12), upper lumbar (L1,2), and lower lumbar (L3-5) and sacral regions. In all 60 patients, each region was scored as involved or not involved by metastases depending on whether the bone scan readings were positive or negative, the readings are tabulated in table-4

The commonest region positive for metastatic involvement, in bone scan, was lower lumbar region with 33 (55%) positive regions and the second commonest was upper lumbar region with 30 positive regions (50%).

Table 5: Bone scan readings as per region

Region	Involved (%)	Not Involved (%)	Total (%)
Cervical	10 (16.7)	50 (83.3)	60 (100)
Upper Thoracic	24 (40)	36 (60)	60 (100)
Lower Thoracic	29 (48.3)	31 (51.7)	60 (100)
Upper Lumbar	30 (50)	30 (50)	60 (100)
Lower Lumbar	33 (55)	27 (45)	60 (100)
Sacral	15 (25)	45 (75)	60 (100)
Total	141(39.2)	219 (60.8)	360 (100)

6. MRI Readings as Per Region

The spine was divided into cervical, upper thoracic (T1-6), lower thoracic (T7-12), upper lumbar (L1-2), and lower lumbar (L3-5) and sacral regions. In all 60 patients, each region was scored as involved or not involved by metastases depending on whether the MRI readings were positive or negative. The readings are tabulated in Table 6.

Table 6: MRI readings as per region

Region	Involved (%)	Not Involved (%)	Total (%)
Cervical	17 (28.3)	43 (71.7)	60 (100)
Upper Thoracic	33 (55)	27 (45)	60 (100)
Lower Thoraci	43 (71.7)	17 (28.3)	60 (100)
Upper Lumbar	43 (71.7)	14 (28.3)	60 (100)
Lower Lumbar	46 (76.7)	14 (23.3)	
Sacral	21 (35)	39 (65)	60 (100)
Total	203 (56.4)	157 (43.6)	360 (100)

The commonest region positive for metastatic involvement, in MRI was lower lumbar region with 46 (76.7%) positive regions. The lower thoracic and upper lumbar regions were the second commonest with 43 (71.7%) positive regions each.

7. Comparison of Regions Read Positive and Negative on Bone Scan And MRI

Table 7 summarizes the comparison of regions read positive or negative on bone scans and MRI.

Table 7: Comparison of regions read positive and negative

Region	BS+ MRI+	BS- MIR-	BS+ MRI-	BS- MRI+	Total
Cervical	10	43	0	7	60
Upper Thoracic	23	26	1	10	60
Lower Thoracic	28	16	1	15	60
Upper Lumbar	28	15	2	15	60
Lower Lumbar	30	11	3	16	60
Sacral	14	38	1	7	60
Total	1233	149	8	70	360

BS-Bone scan, MRI- Magnetic Resonance Imaging

Of the 360 regions, 133 regions (36.9%) were read positive on both bone scan and MRI and 149 regions (41.4%) were read negative on both. 8 regions (2.2%) were read positive on bone scan and negative on MRI and 70 (19.5%) regions were read positive on MRI and negative on bone scan.

8. Concordant and discordant regions

Table 8 summarizes the concordance, or lack of it, in regions read positive or negative on bone scans and MRI. The regions were read as concordant if the readings were positive or negative on MRi and bone scan combined and discordant if otherwise. 282 regions (78.3%) were read as concordant on bone scan and MRI and 78 regions (21.7%) were read as discordant.

Table 8: MRI readings as per region

Region	Concordant regions (%)	Discordant Regions (%)	Total
Cervical	53 (88.3)	7 (11.7)	60
Upper Thoracic	49 (81.7)	11 (18.3)	60
Lower Thoraci	44 (73.3)	16 (26.7)	60
Upper Lumbar	46 (76.7)	14 (23.3)	60
Lower Lumbar	41 (68.3)	19 (31.7)	60
Sacral	21 (35)	39 (65)	60
Total	203 (56.4)	157 (43.6)	360

X^2 chi square value = 12.37   Degrees of freedom = 5   P value = 0.03

The discordance was commonest in lower lumbar region with 19 regions (31.75). Upper lumbar region was the second commonest discordant region with 17 regions (28.3)

9. Discordant readings by region as per primary in specific cancers

The discordant regions were further evaluated in the three commonest primary tumors, that is carcinoma breast, prostrate and lung.

I. Discordant regions in carcinoma breast patients.

In the 19 patients of carcinoma breast, the commonest region to be involved by metastases was upper lumbar region (involved in 15 patients). The second commonest region involved was lower lumbar region (involved in 11 patients.).

A total of 25 regions were read as discordant in the 19 patients of carcinoma breast. 2 (8%) regions were read as positive on bone scan and negative on MRI. 23(92%) regions were read as positive on MRI and negative on bone scan. The discordance was the maximum in the upper lumbar region with 7 regions (285). Lower lumbar regions was the second commonest discordant region with 6 regions (24%). Table 9 shows the distribution of discordant regions in patients of carcinoma breast.

Table 9: Discordant regions in carcinoma breast patients

Region	Bone Scan = MRI-(%)	Bone Scan- MRI+ (%)	Total (%)
Cervical	0 (0)	1 (4)	1 (4)
Upper Thoracic	0 (0)	3 (12)	3 (12)
Lower Thoraci	0 (0)	5 (20)	5 (20)
Upper Lumbar	1 (4)	6 (24)	7 (28)
Lower Lumbar	1 (4)	5 (20)	6 (24)
Sacral	0 (0)	3 (12)	3 (12)
Total	2 (8)	23 (92)	25 (100)

II. discordant regions in carcinoma prostrate patients

In the 16 patients of carcinoma prostrate, the commonest region to be involved by metastases was lower lumbar region (involved in 13 patients). The second commonest region involved was sacral region (involved in 9 patients)

Table -10 shows the distribution of discordant regios in patients of carcinoma prostrate, 2 regions (9.6%) were read as positive on bone scan and negative on bone scan. The discordance was the maximum in the lower lumbar region, with 7 regions (33.3%)

Table 10: Discordant regions in carcinoma prostrate patients

Region	Bone Scan = MRI-(%)	Bone Scan- MRI+ (%)	Total (%)
Cervical	0 (0)	1 (4.8)	1 (4.8)
Upper Thoracic	0 (0)	1 (4.8)	1 (4.8)
Lower Thoraci	0 (0)	3 (14.3)	3 (14.3)
Upper Lumbar	0 (0)	4 (19)	4 (19)
Lower Lumbar	1 (4.8)	6 (28.5)	7 (33.3)
Sacral	1 (4.8)	4 (19)	5 (23.8)
Total	2 (8)	23 (92)	25 (100)

III. Discordant regions in carcinoma lung patients

In the 9 patients of carcinoma lung, the commonest region to be involved by metastases was lower thoracic region (involved in 6 patients). The second commonest region involved was upper lumbar region (involved in 5 patients)

1 region (8.35) was read as positive on bone scan and negative on MRI, 11 regions (91.7%) were read as positive on MRI and negative on bone scan. The discordance was the maximum in the lower thoracic region, with 5 regions (41.6%)

Table 11: Discordant regions in carcinoma lung

Region	Bone Scan = MRI-(%)	Bone Scan- MRI+ (%)	Total (%)
Cervical	0 (0)	1 (8.3)	1 (8.3)
Upper Thoracic	0 (0)	1 (8.3)	1 (8.3)
Lower Thoracic	1 (8.3)	4 (33.3)	5 (41.6)
Upper Lumbar	0 (0)	3 (25)	3 (25)
Lower Lumbar	0 (0)	2 (16.7)	2 (16.7)
Sacral	0 (0)	0 (0)	0 (0)
Total	1 (8.3)	11 (91.7)	12 100)

Total number of vertebrae involved by metastases

In the 60 patients evaluated in our study, a total of 1740 vertebrae were studied. Table 12 shows the number of vertebrae positive and negative on bone scan and MRI respectively.

Table 12: Number of vertebrae involved by metastases

MRI	Bone Scan		Total (%)
	Positive	**Negative**	
Positive	274 (15.7)	90 (5.2)	364 (20.9)
Negative	10 (0.6)	1366 (78.5)	1376 (79.1)
Total	284 (16.3)	1456 (83.7)	1740 (100)

1366 (78.5) vertebrae were read as negative on both modalities. 374 (21.5%) vertebrae were read as positive on MRI or bone scans. 364 (20.9%) vertebrae were positive on MRI and 284 (16.3%) vertebrae were positive on bone scan. 274 (15.7%) vertebrae were read as positive on both bone scan and MRI. 90 (5.2%) vertebrae were read as positive on MRI and negative on bone scan. 10 (0.6%) vertebrae were read as positive on bone scan and negative on MRI.

10.correlation of positive bone scan with lesion size on MRI

The size of each lesion in 364 vertebrae, that were read as positive on MRI, was measured at its greatest dimension on MRI. The lesions were categorized as small (<2 cm) or large (>2 cm) and the results are tabulated in Table 13.

Table 13: Correlation of positive bone scans with lesion size on MRI

Size on MRI	Bone Scan reading		Total (%)
	Positive (%)	**Negative(%)**	
Small (<2 cms)	2 (2.4	80 (97.6)	82 (100)
Large (>2cms)	272 (96.5)	10 (3.5)	282 (100)
Total	274 (75.3)	90 (27.7)	364 (100)

X^2 chi square value = 301.69   Degrees of freedom = 15   P value = 0.0000

274 vertebrae (75.3) were read as positive on bone scan and 90 vertebrae (24.7%) negative. 82 small lesions (22.5%) and 282 large lesions (77.5%) were identified in the 364 vertebrae. Out of the 82 small lesions, only 2 lesions (2.4%) were read as positive and 80 lesions (97.6%) were read as negative. Out of the 282 large lesions. 272 lesions (96.55) were read as positive and 10 lesions (3.5%) were read as negative.

**11. Correlation of positive bone scan with lesion location on MRI**

The lesions in all 364 vertebrae, that were read as positive on MRI, were classified as intramedullary, subcortical and transcortical. This was based on the

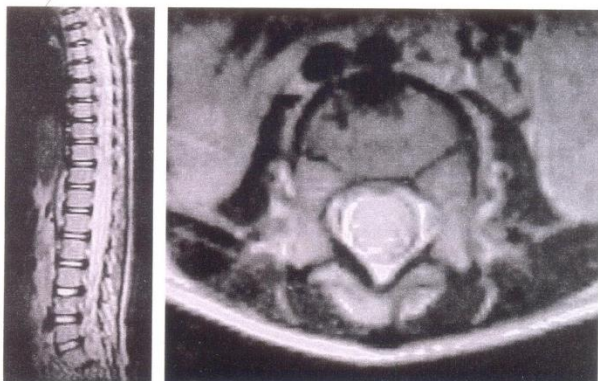relationship between the lesion and cortical bone. The results are tabulated in Table 14.

274 vertebrae (75.35) were read as positive on bone scan and 90 vertebrae)25.75) negative. 70 intramedullary (19.2%), 76 subcortical (20.8%) and 218 transcortical (605) lesions were identified in the 364 vertebrae. Out of the 70-intramedullary lesions, none of the lesions (0%) were positive on bone scan. Out of the 76 subcortical lesions, 58 lesions (76.3%) lesions were positive on bone scan and 18 lesions (23.75) were negative. Out of the 218-transcortical lesions, 216 lesions (99.1%) were positive on bone scan and 2 lesions (0.9%) were read as negative.

Table 14: Correlation of positive bone scans with lesion location on MRI
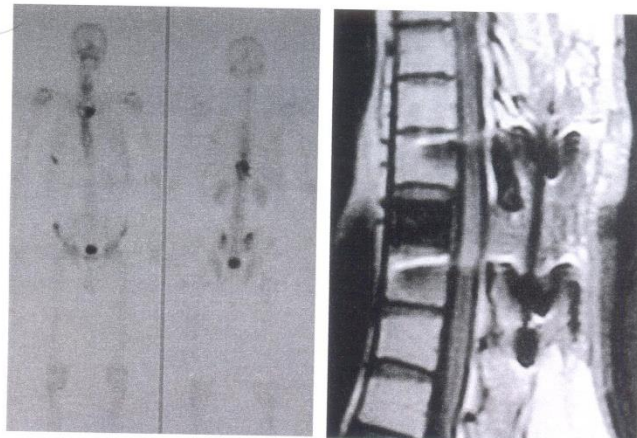
| Location on MRI	Bone Scan reading		Total (%)
	Positive (%)	**Negative(%)**	
Intramedullary	0(0)	70 (100)	70 (100)
Subcortical	58 (76.3)	18 (23.7)	76 (100)
Transcortical	216 (99.1)	2 (0.9)	218 (100)
Total	274 (75.3)	90 (25.7)	364 (100)
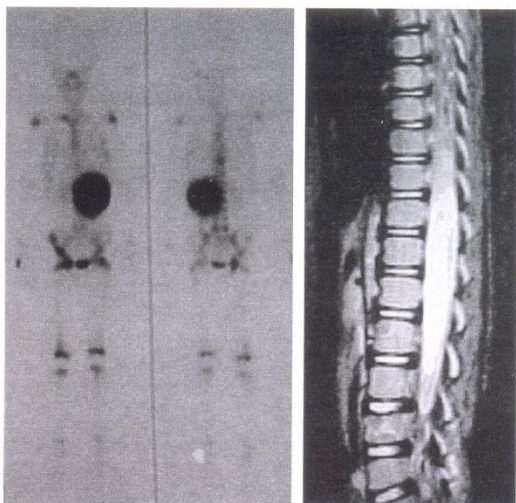
Case of Neuroblastoma stage III, in a 03 years old boy.
Bone scan showing the large intra-abdominal lesion and increased uptake in DV9.
STIR sagittal image of the dorsolumbar spine showing hyperintense lesions in DV9 and LV4.


Case of Carcinoma lung in a 48 years old man with compression fracture DV10 (operated).
Bone scan showing increased uptake in DV10.
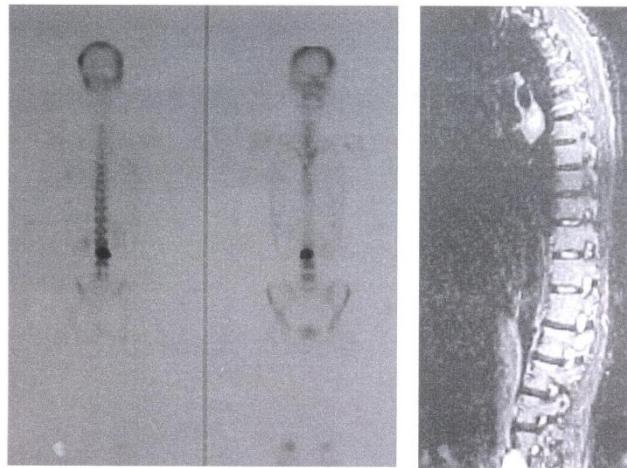T1- weighted image of the dorsal spine showing collapse of DV10 with spinal stabilizers in DV9 and LV11. The vertebral marrow of DV10 appears hypointense.
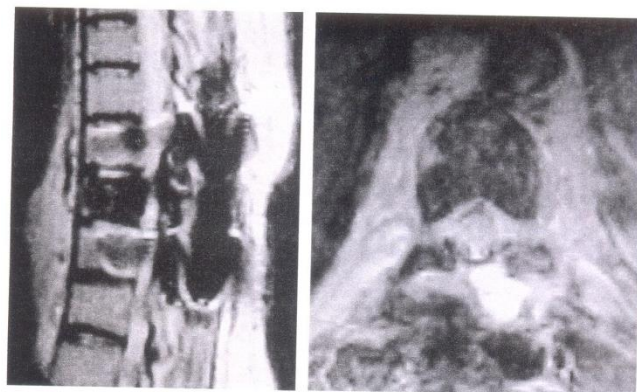
T2- weighted sagittal image of the dorsolumbar spine showing hyperintense lesions in DV9 and LV4.
T1- weighted axial image at the level of LV4 showing large subcortical lesion.

T2- weighted image of the dorsal spine showing collapse of DV10 with spinal stabilizers in DV9 and LV11.
T1- weighted axial image at the level of DV10 showing hypointense marrow of DV10, suggestive of replacement of the marrow by metastatic tumor tissue.
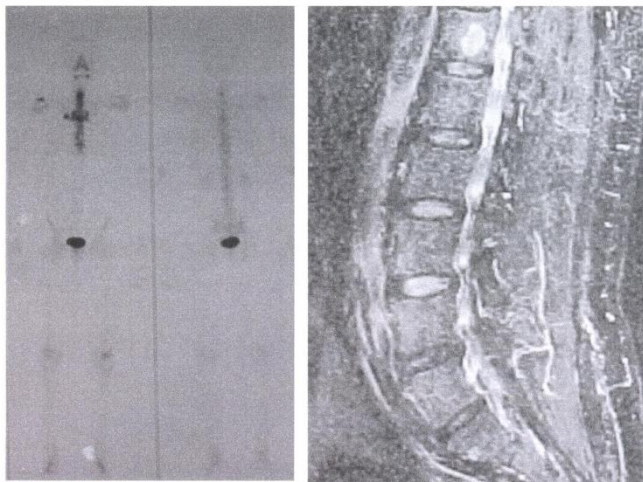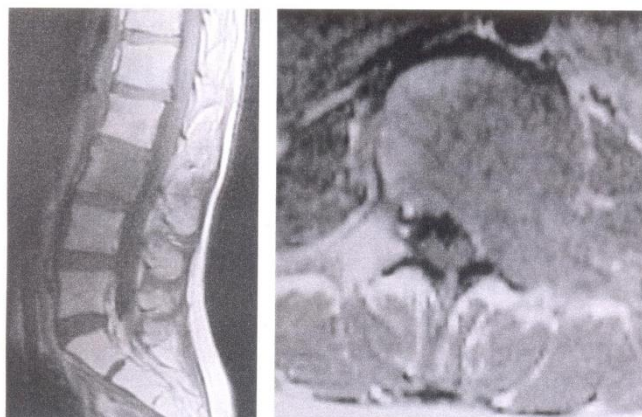
Case of carcinoma prostrate, in a 66 years old man.
Normal bone scan.
STIR sagittal image of the lumbosacral spine showing hyperintense lesion in
LV1.
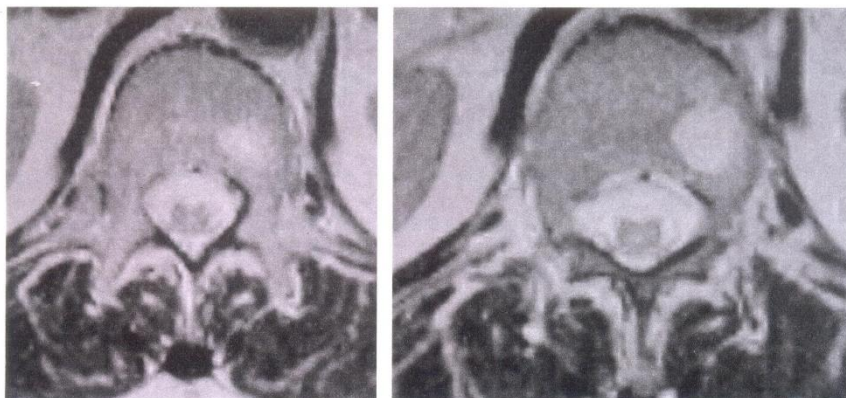
T2- weighted axial image at the level of LV1 showing large hyperintense
subcortical lesion.
Post contrast T1- weighted axial image at the level of LV1 showing intense
enhancement of the lesion.

Case of melanoma, in a 24 years old lady.
Bone scan showing increased uptake in LV3.
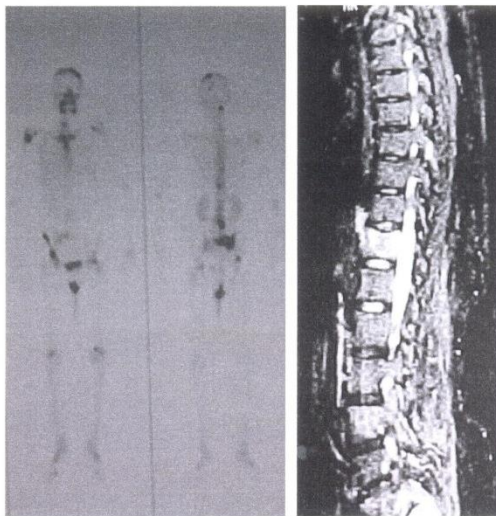STIR sagittal image of the whole spine showing hyperintense lesion in LV3.

T1- weighted sagittal image of the lumbosacral spine showing hypointense lesion in LV3.
T1- weighted axial image at the level of LV3 showing large transcortical lesion in LV3.
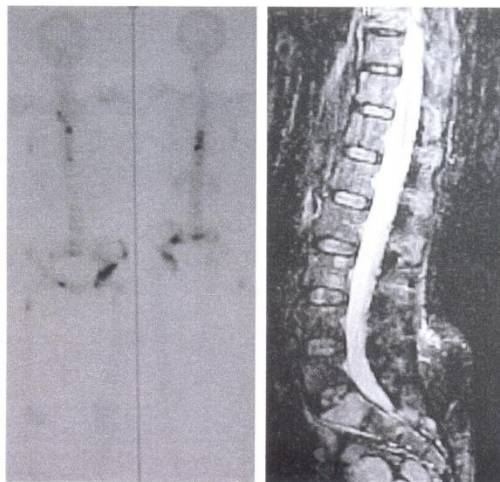
Case of carcinoma thyroid, in a 47 years old lady.
Bone scan showing increased uptake in DV 7, 8, S1, left innominate bone and right superior pubic ramus.
STIR sagittal image of the dorsolumar spine showing hyperintense lesions in DV7, 8, 9, LV3 and SV1.
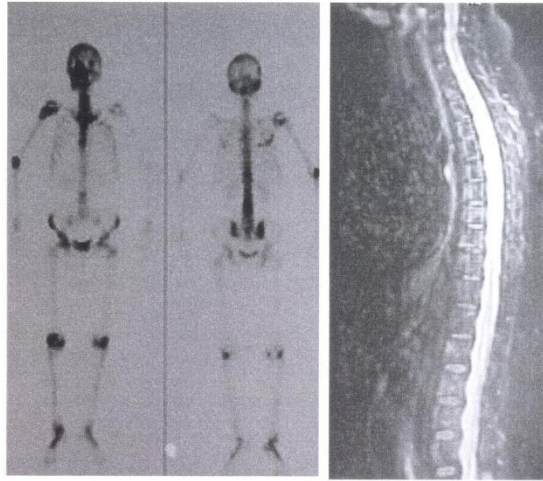

T2- weighted image of the whole spine showing hyperintense lesions in DV 7,8,9 and LV3.
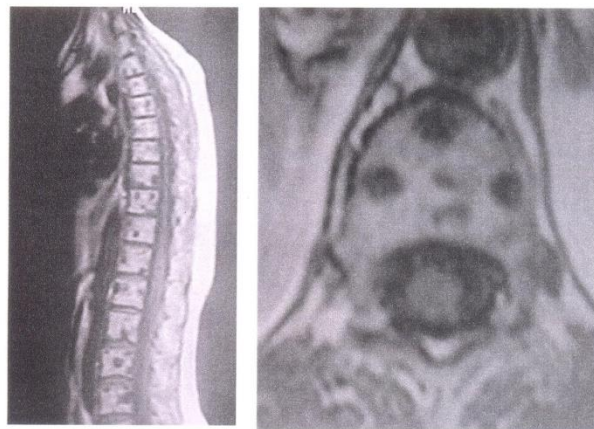T1- weighted axial image at the level of DV9 showing multiple small intramedullary lesions.

Case of carcinoma breast, in a 65 years old lady.
Bone scan showing increased uptake in DV12, LV4, SV1, Skull, right humerus and right innominate bone.
STIR sagittal image of the dorsolumbar spine showing hyperintense lesions in DV12, LV4, SV1 and SV2.

T1- weighted sagittal image of the lumbar spine showing hypointense lesions in DV12 and LV4.
T2- weighted axial image at the level of LV4 showing large transcortical lesion.

Case of carcinoma prostrate, in a 66 years old man.
Bone scan showing increased uptake in DV10, LV1, 2, 5 and both innominate bones.
STIR sagittal image of the whole spine showing hyperintense lesions in DV6 to 12 and LV1,2 and LV5 .


T1- weighted sagittal image of the whole spine showing hypointense lesions in DV6 to 12 and LV1,2 and LV5 .
T1- weighted axial image at the level of DV12 showing multiple small intramedullary and subcortical lesions.

Case of carcinoma breast, in a 59 years old lady.
Bone scan showing increased uptake in DV8, 11, 12, LV5 and innominate bones.
STIR sagittal image of the dorsolumbosacral spine showing hyperintense lesions
in DV8, 9, 11, 12, LV3, 4, 5 and SV1.
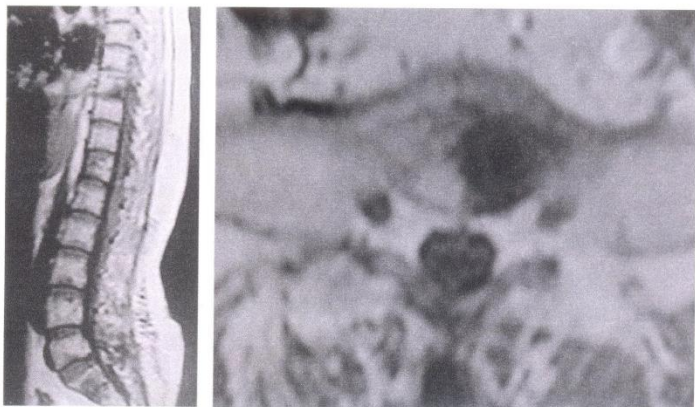
T1- weighted image of the dorsolumbosacral spine showing hypointense lesions
in DV8, 9, 11, 12, LV3, 4, 5 and SV1.
T1- weighted axial image at the level of SV1 showing large subcortical lesion.
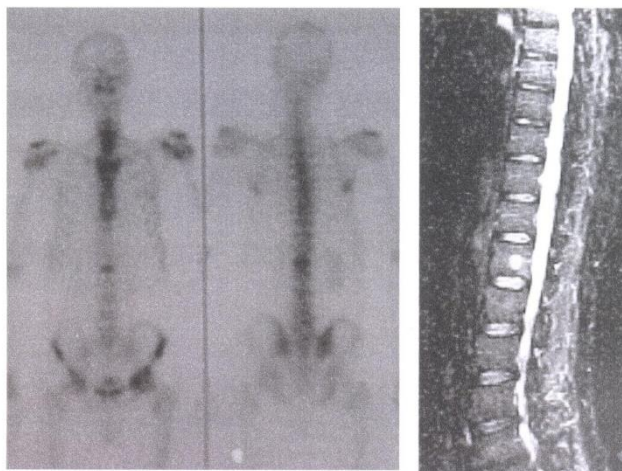
Case of carcinoma lung, in a 61 years old man.
Bone scan showing increased uptake in LV1.
STIR image of the lumbosacral spine showing hyperintense lesion in LV1.
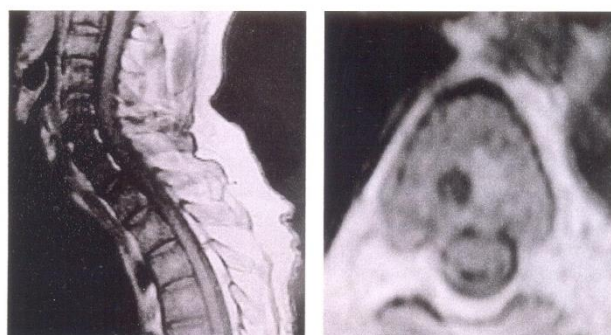
T1- weighted image of the cervicdorsal spine showing hypointense lesions in
DV5 and DV6.
T1- weighted axial image at the level of DV5 showing small intramedullary lesion.

DISCUSSION

In our study, 60 patients with a proven malignancy and clinical and laboratory suspicion of vertebral metastases were included between the ages of 14 months to 71 years. The mean age of the patients was 46 years and 32 males (53.3) and 28 females (46.7%) formed part of our study. The commonest age group of patients with vertebral metastases was 51-60 years. This was in consonance with the finding of various authors as mentioned in Table 2.

Table 15: Commonest age group of patient with vertebral metastases

Sl. No	Study	Year	Commonest age group
1.	Avrahami E *et al* [35]	1989	51-60 years
2.	Frand JA [39]	1990	51-60 years
3.	Taoka T [1]	2001	51-60 years
4.	Our study	2005	51-60 years

The commonest primary tumor in our study was carcinoma breast with 19 cases (31.7%). Various authors have also reported similar frequency of primary tumors, as mentioned in Table 2.

Table 16: Frequency of commonest primary tumor

Sl. No	Study	Year	Commonest age group
1.	Avrahami E *et al* [35]	1989	Carcinoma Breast
2.	Frand JA [39]	1990	Carcinoma Breast
3.	Taoka T [1]	2001	Carcinoma Breast
4.	Our study	2009-2010	Carcinoma Breast

The second commonest tumor in our study was carcinoma prostrate with 16 cases (26.7%). Carcinoma lung was the third commonest with 9 cases (15%).

Carcinoma breast was commonest in the age group between 41-50 years with 7 cases (36.8%). Carcinoma prostrate was commonest in the age group between 51-60 years with 7 cases (43.8%). Carcinoma lung was commonest in the age group between 41-50 years with 3 cases (33.3%).

Out of the total 360 regions, bone scan was positive in 141 regions (39.2%) and negative in 219 regions (60.8%). The commonest region positive for metastatic involvement, in bone scan, was lower lumbar region with 33 (555) positive regions and the second commonest was upper lumbar region with 30 positive regions (505). This was comparable to the previous studies as shown in Table 3.

Table 17: Commonest region positive for metastases in bone scan

Sl. No	Study	Year	Commonest regions	Second commonest
1.	Gosfield E III *et al* [41]	1993	Lower lumbar	Upper lumber
2.	Cesani F *et al* [44]	1995	Lower lumbar	Upper lumber
3.	Our study	2009-2010	Lower lumbar	Upper lumbar

Out of the total 360 regions, MRI was positive in 203 regions (56.4%) and negative in 157 regions (43.6%)

Table 18: Commonest region positive for metastases in MRI

Sl. No	Study	Year	Commonest regions	Second commonest
1.	Gosfield E III *et al* [41]	1993	Lower lumbar	Upper lumber
2.	Cesani F *et al* [44]	1995	Lower lumbar	Upper lumber
3.	Our study	2009-2010	Lower lumbar	Upper lumbar, lower thoracic

The commonest region positive for metastatic involvement, in MRI, was lower lumbar region with 46 (76.7%) positive regions, this was comparable to the previous studies as shown in Table 4.

The lower thoracic and upper lumbar regions were the second commonest with 43 (71.7%) positive regions each, whereas in other studies upper lumbar region was the only second commonest region. This minor variation in our finding may be explained on the basis of small sample size of our study.

Of the 360 regions 133 regions (36.9%) were read positive on both bone scan and MRI and 149 regions (41.4%) were read negative on both. 8 regions (2.2%) were read positive on bone scan and negative on

MRI and 70 (19.5%) regions were read positive on MRI and negative on bone scan.

More patients were absolutely and relatively considered to have metastatic involvement of the spine by MRI than by bone scan. Overall, the distribution of positive regions was similar on bone scans and MRI with the greatest number in the lower lumbar region and the least in the cervical region.

The discordance was commonest in lower lumbar region with 19 regions (31.7%). Upper lumbar region was the second commonest discordant region with 17 regions (28.3%). The difference between proportions of discordant readings was found to be statistically significant (p=0.03). our findings are in

consonance with the findings of various authors as mentioned in Table-5

Table 19: Commonest discordant region

Sl. No	Study	Year	Commonest discordant region
1.	Gosfield E III et al[41]	1993	Lower lumbar
2.	Cesani F et al [44]	1995	Lower lumbar
3.	Our study	2009-2010	Lower lumbar

Our findings of great discordance in the lumbar region (36 out of total 78 discordant regions – 46.2%) may be due to the composition of the study population. Lumbar spine metastases are common in breast (upper lumbar region) and prostrate cancer patients (lower lumbar region), the two groups comprising the preponderance of our patients sample. The discordance may be related to the pattern of physiological spread in these two types of malignancy. Carcinoma breast and prostrate commonly spread through Batson's venous plexus. Batson's plexus is a low pressure, valveless system with multiple venous communications throughout the thoracolumbar spine and pelvis [61].

Carcinoma Breast

Breast cancer metastases can be osteoblastic, osteolytic, or mixed.Bone is the most common site for metastases and the lesions are primarily found in the axial skeleton. Unfortunately, bone metastases from breast carcinoma can occur many years after the initial diagnosis. 21% of patients with distant relapse in bone have a single metastatic deposit, with the spine being the most common site [66]. Metastasis is common to the L-2 vertebral body.

Initial studies reported that a significant number of patients with early stage disease (stage I and II) had bone metastases. Recent, more rigorous, evaluation has shown that essentially only those patients with aggressive stage II disease have bone involvement [67]. The number and distribution of metastases can provide prognostic information, with patients harboring less than three new lesions surviving longer. Conversion to a positive bone scan holds a poor prognosis.

In the 19 cases of carcinoma breast in our study, the commonest age group was 41 to 50 years. The commonest region to be involved by metastases was upper lumbar region (involved in 15 patients, 78.9%). The second commonest region involved was lower lumbar region (involved in 11 patients, 57.9%). This was in consonance with the findings of Gosfield E III *et al* [41] and Resnick D *et al* [68].

A total of 25 regions were read as discordant in the 19 patients of carcinoma breast. 2 (8%) regions were read as positive on bone scan and negative on MRI. 23 (92%) regions were read as positive on MRI and negative on bone scan. The discordance was the maximum in the upper lumbar region with 7 regions (285). This is possibly because upper lumbar region is the commonest region to be involved by metastases in carcinoma breast patients. Lower lumber regions was the second commonest discordant region with 6 regions (24%). Various authors have also reported similar findings.

Table 20: Commonest discordant region in Carcinoma Breast patients

Sl. No.	Study	Year	Commonest discordant region
1.	Gosfield E III *et al* [41]	1993	Upper lumbar
2.	Cesani F *et al* [44]	1995	Upper lumbar
3.	Our study	2009-2010	Upper lumbar

Carcinoma prostrate frequently metastasizes to bone, often as its first site, distributing primarily to the axial skeleton (particularly the spine and pelvis). Bulky metastatic disease can be present before patient die from their disease. There is prolonged patient survival when metastases number fewer than six, are confined to the axial skeleton, and do not involve the skull or sternum [69].

In the 16 cases of carcinoma prostrate in our study, he commonest age group was 51 to 60 years. The commonest region to be involved by metastases was lower lumbar region (involved in 9 patients, 56.3%). This was in consonance with the findings of Gosfield E III *et al* [41] and Resnick D *et al* [69].

A total of 21regions were read s discordant in the 16 patients of carcinoma prostrate. 2 (9.6%) regions were read as positive on bone scan and negative on MRI. 19 (19.4%) regions were read as positive on MRI and negative on bone scan. The discordance was the maximum in the lower lumbar region with 7 regions (33.3%). This is possibly because lower lumbar region is the commonest region to be involved by metastases in

carcinoma prostrate patients. Sacral region was the second commonest discordant region with 5 regions (23.8%). Various authors have also reported similar findings.

Table 21: Commonest discordant region in Carcinoma Prostrate patients

Sl. No.	Study	Year	Commonest discordant region
1.	Gosfield E III *et al* [41]	1993	Lower lumbar
2.	Cesani F *et al* [44]	1995	Lower lumbar
3.	Our study	2009-2010	Lower lumbar

Carcinoma lung

Lung carcinomas can produce an osteolytic, osteoblastic, or a mixed response in bone. Lesions are often seen in T-12 verteba. Small cell lung carcinomas can spread to the bone early, and metastases are often present when the patient is initially evaluated. Bone scanning in patients with lung carcinomas may show focal tracer uptake in the primary tumor mass itself.

Most clinicians feel that routine bone scanning is unnecessary in patients with non-small cell lung carcinoma once either CT or MRI has found metastases in the mediastinum. Patients with metastatic bone disease often exhibit other clinical indicators such as symptoms, or elevated alkaline phosphatase or calcium. Because many patients with these findings do not have metastatic disease, bone scanning and MRI should be reserved for when these clinical parameters are abnormal.

In the 9 cases of carcinoma lung in our study, the commonest age group was 41 to 50 years. The commonest region to be involved by metastases was lower thoracic region (involved in 6 patients, 66.7%). The second commonest region involved was upper lumbar region (involved in 5 patients, 55.6%). This was in consonance with the findings of Gosfield E III *et al* [41] and Resnick D *et al* [69].

A total of 12 regions were read as discordant in the 9 patients of carcinoma lung. 1 (8.3%) regions were read as positive on bone scan and negative on MRI. 11 (91.7%) regions were read as positive on MRI and negative on bone scan. The discordance was the maximum in the lower thoracic region with 5 regions (41.6%). This is possibly because lower thoracic region is the commonest region to be involved by metastases in carcinoma lung patients. Upper lumbar region was the second commonest discordant region with3 regions (25%). Gosfield E *et al* [63] have reported similar findings in their study.

Number of vertebrae involved by metastases

A total of 1740 vertebrae were evaluated in our study of 60 patients. 1366 (78.5%) vertebrae were read as negative on both modalities. 374(21.5%) vertebrae were read as positive on MRI or bone scans. 364 (20.9%) vertebrae wee positive on MRI and 284

(16.3%) vertebrae were positive on bone scan. 274 (15.7%) vertebrae were read as positive on both bone scan and MRI. 90 (5.2%) vertebrae were read as positive on MRi and negative on bone scan. 10 (0.6%) vertebrae were read as positive on bone scan and negative on MRI. The reasons for false negative MRI could not be evaluated in our study.

MR imaging is a sensitive method of detecting intramedullary metastases to those bones with large marrow cavities such as vertebral bodies[4]. However, it is not cost-effective in examining bones with small marrow cavities, such as ribs, because it cannot globally examine the entire skeletal system as bone scintigraphy can. The extra-vertebral metastases (detected by bone scan) were therefore not evaluated by MRI in our study.

The sensitivity of MRI in respect of bone scan, in detection of vertebral metastases, was 97% and the specificity was 94%. This was comparable to the previous study of Eustace S *et al* [48], who also reported a sensitivity of 96.5%

Correlation of positive bone scan with lesion size on MRI

The size of each lesion in 364 vertebrae, that were read as positive on MRI, was measured at its greatest dimension on MRI and the lesions were categorized as small (<2 cm) or large (>2 cm). 82 small lesions (22.5%) and 282 large lesions (77.5%) were identified in the 364 vertebrae. Out of the 82 small lesions, only 2 lesions (2.4%) were read as positive and 80 lesions (97.6%) were read as negative. Out of the 282 large lesions, 272 (96.5%) were read as positive and 10 lesions (3.5%) were read as negative.

Percentage of small sized lesions diagnosed by bone scan was significantly lower than the percentage of large size lesions diagnosed. Pearson's chi-square test (x^2 Chi square value = 301.69) confirmed a statistically highly significant correlation between the lesion size and bone scintigraphci results (p value = 0.0000). this was in consonance with previous study of Taoka T *et al* [1].

Because the vertebral body has a relatively large marrow cavity, early or small metastases tend to be intramedullary without cortical involvement [4] and

may not cause sufficient bony remodeling to be detected on bone scans. Small lesions or lesions localized away from the cortex are, therefore, likely to be undiagnosed on bone scintigraphy, despite destruction of trabecular bone. Even if most of the bone marrow has been infiltrated with metastases, the uptake of radioactive tracers caused by the destruction with metastases, the uptake of radioactive tracers caused by the destruction of the relatively small amount of medullary boney matrix remains low and, therefore, may not be easily appreciated when the uptake is contrasted with that of the normal cortex.

Correlation of positive bone scan with lesion location on MRI

The lesions in all 364 vertebrae, that were read as positive on MRI, were classified as intramedullary, subcortical and transcortical. This was based on the relationship between the lesion and cortical bone. 70intramedullary (19.2%). 76 subcortical (20.8%) and 218 transcortical (60%) lesions were identified in the 364 vertebrae. Out of the 70-intramedullary lesions, none of the lesions (0%) were positive on bone scan. Out of the 76 subcortical lesions, 58 lesions (76.3%) lesions were positive on bone scan and 18 lesions (23.7%) were negative. Out of the 218-transcortical lesions, 216 lesions (99.1%) were positive on bone scan and 2 lesions (0.95) were read as negative.

Percentage of intramedullary and subcortical lesions diagnosed by bone scan was significantly lower than the percentage of transcortical lesions diagnosed. Pearson's chi-square test (X^2 Chie square value + 301.69) confirmed a statistically highly significant correlation between the lesions size and bone scintigraphic results (p value = 0.0000). this was in consonance with previous study of Taoka T *et al* [1].

The mechanism of abnormal Tc-99m MDP uptake shown in bone scanning is complex. Abnormal radionuclide uptake is generally believed to increase with regional bone-blood flow, bone remodeling, formation of new bone, and enhanced bone matrix turnover [1,58]. Bone scintigraphy is sensitive for detecting areas of bone remodeling, particularly cortex. However, abnormal increase of uptake in the medullary cavity because of tumor destruction of the medullary bony matrix may not be as obvious because of the relatively small amount of medullary bone and relatively high uptake of the normal cortical bone.

MR imaging is a sensitive method of detecting intramedullary metastases in vertebral bodies. Our findings suggest that cortical involvement is likely to key factor contributing to the difference in detection rates of vertebral body metastases on MRI and bone scintigraphy and that MRI is a sensitive and specific modality in detection of vertebral metastases.

CONCLUSION

Total of 60 patients (between the ages of 14 months of 71 years) with a proven malignancy and clinical and laboratory suspicion of vertebral metastases were evaluated on radionuclide bone scan and MR imaging. Male : female ratio was 1:1.14. the commonest age group of patients with vertebral metastases was 51-60 years.The commonest primary tumor was carcinoma breast (19 patients). Carcinoma prostrate was the second commonest (16 patients) and carcinoma lung the third commonest (9 patients).Of the total 360 evaluated regions, bone scan was positive in 141 regions and negative in 219 regions. The commonest region positive for metastatic involvement, in bone scan, was lower lumbar region (33 regions). Of the total 360 evaluated regions, MRI was positive in 203 regions and negative in 157 regions. The commonest region positive for metastatic involvement, in MRI, was lower lumbar region (46 region) .The discordance between bone scan and MRI was commonest in lower lumbar region (19 regions). Upper lumbar region was the second commonest discordant region (17 regions). The commonest region to be involved by metastases in carcinoma breast patients was upper lumbar region (involved in 15 patients, 78.9%). The commonest discordant region in these patients was upper lumbar with 7 regions read as discordant (28%). The commonest region to be involved by metastases in carcinoma prostrate patients was lower lumbar region (involved in 13 patients, 81.3%). The commonest discordant region in these patients was lower lumbar with 7 regions read as discordant (33.3%).The commonest region to be involved by metastases in carcinoma lung patients was lower thoracic region (involved in 6 patients, 66.7%). The commonest discordant region in these patients was lower thoracic with 5 regions read as discordant (41.6%). Out of the total 1740 vertebrae that were evaluated in our study, 374 vertebrae were read as positive on MRI or bone scans. Of these 374 vertebrae, 364 (97.3%) vertebrae were positive on MRI and 284 (75.9%) were positive on bone scan. The sensitivity of MRI as against bone scan, in detection of vertebral metastases, was 96.5% and the specificity 94%.The correlation of positive bone scan with lesion size of MRI was found to be statistically highly significant (p value =0.0000). percentage of small sized lesions diagnosed by bone scan was significantly lower than the percentage of large size lesions diagnosed. The correlation of positive bone scan with lesions location on MRI was found to be statistically (p value = 0.0000). percentage of intramedullary and subcortical lesions diagnosed by bone scan was significantly lower than the percentage of transcortical lesions diagnosed. MR imaging was found to have a higher sensitivity and specificity as against radionuclide bone scan in early detection of vertebral metastases.

REFERENCES

1. Taoka T, Mayr N, Lee HJ, Yuh WTC, Simonson TM. Factors influencing visualization of vertebral metastases on MR Imaging versus boenscintigraphy. AJR. 2001; 176: 1525-1530.
2. ScutellariPN, AntinolfiG, GaleottiR, Giganti M. Metastatic bone disease: Strategies for Imaging. Minerva Med. 2003; 94:77-90.
3. Yuh WTC, Zachar CK, Barloon TJ, SicketsWj, Hawes DR. Vertebral compression fractures: distinction between beingn and malignant causes with MR Imaging. Radiology. 1989; 172:215-218.
4. Yuh WT, Quests JP, Lee HJ. anatomic distribution of metastases in the vertebral body and modes of hematogenous spread. Spine. 1996; 21: 2243-2250.
5. Aitchison F, Poon FW, Hadley MD, Gray HW, Forrester AW. Vertebral metastases and an equivocal bone scan : value of MRI. Nucl Med commun. 1992; 131:429-431.
6. Thrall TH, Ellis Bl. Skeletal metastases. RadiolClin North Am. 1987; 25:1155-1170.
7. Dickison F, Liddicoaat A, Dhingsa R. MRI versus radionuclide scintigraphyofor screening in bone metastases. ClinRadiol. 2000; 55 (8):653
8. Shin WJ. Vertebral SPECT bone scintigraphshuld be compared with MRI for vertebral metastases. AJR. 2001; 177:1482.
9. Attenhoefer C. Ghanem M, Moger E. Comparative detectability of bone metastases & impact on therapy of MRI and bone scintigraphy in patients with breast cancer. Eur J Rardiol. 2001; 40: 16-23.
10. Shih WJ. Runge VV, Mitchell LB. comparsion of bone SPECT, MRI & in the demonstration of vertebral metastases from bronchogenic carcinoma: an autopsy-docummented case. ClinNucl Med. 2000; 25 (8) : 647-649.
11. Porte BA, Olson DO, Stimac GK, Shields AR, Nelson SJ. STIR Imaging marrow malignancies. In : Proceedings of the annual meeting SocMagnReson Med. 1987;1:146.
12. Porter BA, Shields AF, Olson DO. Magnetic resonance Imaging of bone marrow disorders. RadiolClin North Am. 1986; 24:269-289.
13. Stimac GK, Porter BA, Oison DO. Gerlach R, Genton M. Gadolinium-DTPA- enhanced MR imaging of spinal neoplasms: preliminary investigation and comparison with unehance spine-echo and STIR sequences. AJR. 1988 Dec; 151(6):1185-1192.
14. Cassen B, Curtis W, Reed C. Instrumentation for 131l use in medical studis. Nucleonic. 1951; 2: 46.
15. Anger HO. Use of gamma-ray pin-hole camea for in vivo studies. Nature. 1952; 170:200.
16. Neuman WF, Neuman MW. The nature of the mineral phase of man. Chem. Rev. 1953; 53.1.
17. Fleisch H, Bisaz S. Isolation from urine of pyrophosphate, a calcification inhibitor. Am J Physiol. 1992; 165:911.
18. Fleisch H, Irving JT, Schilbler D. Bone formation in normal and vitamin D treated rachitic rats during the administration of polyphosphates. Proc. SocExpBiol Med. 1966;123:332.
19. Fleisch H, Russel RG, Francis MD. Diphosphonates inhibit hydroxypatitle dissolution in vitro and bone resorption in tissue culture and in vivo. Science. 1969; 165:1262.
20. King WR, Francis MD, Michael WR. Effect of disodium ethanyl-1-hydroxy, 1,1-diphosphonate on bone formation. ClinOrthop. 1971; 78:251.
21. Subramanian G, McAfee JG. A new complex of 99m Tc for skeletal imaging. Radiology. 1971; 99:192.
22. Subramanian G. McAfee JG, Blair RJ. 99m Tc_EHDP : a potential radiopharmaceutical for skeletal imaging. J Nucl Med. 1972; 13:947.
23. Bloch FO, Hansen WW. Packard ME. Nuclear induction. Phy Rev. 1946; 69:127.
24. Purcell ENM, Torrey HC. Pound CV. Resonance Absorption by Nuclear magnetic Movements in a solid. Phy. Rev. 1946; 64:37-38.
25. Brasch RC. Methods of contrast enhancement for NMR imaging and potential applications. Radiology, 1983; 147:781-783.
26. Mendonca-Dias MH, Gagelli E, Lauterbeur PC. Paramagnetic contrast against in NMR medical imaging. SeminNucl Med. 183; 13:364-376.
27. Runge VM, Clanton et al. intravascular contrast agents suitable for magnetic resonance imaging. Radiology. 1984 ; 153:171-176.
28. Carr DH, Brown J. Gadolinium-DTPA as contrast agent in MRIU: initial clinical experience in 20 patients. AJR. 1984; 143:215-225.
29. Haughton VM, Rimm AA, Czervinoke LF. Sensitivity of Gadolinium-DTPA enhanced MR imaging of benign extra-axial tumors. Radiology. 1988; 166:829-833.
30. Felix R, Schomer W, Laniado M. bran tumors: MR Imaging with Gadolinium-DTPA. Radiology. 1985; 156:681-688.
31. Brant-Zawadzki M, Berry I, Osaki L. Gadolinium-DTPA in clinical MR of the Brain in intra-axial lesions. AJNR. 1986;7:781-788.
32. Russell EJ, Geremia GK, Johnson CE. Multiple Cerebral metastases: detect ability with gadolinium-DTPA enhanced MR Imaging. Radiology. 1987; 165:609-617.
33. Vanel D, Couanet D, Leclere J. Patte C. Early detection of bone metastases of Ewing's sarcoma by magnetic resonance imaging. Diagn Imaging Clin Med. 1985; 55(6): 381-3.
34. Delbeke D, Powers TA, Sandler MP. Correlative radionuclide and Magnetic Resonance Imaging in the evaluation of the spine. ClinNucl Med. 1989; 14:742-49.
35. Avrahami E, Tadmor R, Dally O, Hadar H. Early MR demonstration of spinal metastases in patients

with normal radiographs and CT and radionuclide bone scans. J Comput Assist Tomogr. 1989; 13:598-602.

36. Kattapuram SV, Khurana JS, Scott JA. Negative scintigraphy with positive MRI in bone metastases. Skeletal Radiol. 1990; 19:113-116.

37. Dicuonzo F, Farchi G, Lorusso A, Palma M. Staging of spinal metastasis using special techniques of magnetic resonance imaging. Radiol Med (Torino). 1990 Dec; 80(6): 818-22.

38. Jelinek JS, Redmond J, Perry JJ.small cell lung cancer: Staging with MR Imaging Radiology. 1990 Dec; 177(3) : 837-842.

39. Frank JA, Ling A, Patronas NJ. Detection of malignant bone tumors: MR imaging vs scintigraphy. AJR. 1990 Nov; 155 (4):1043-48.

40. Ruzal-Shapiro C, Berdon WE, Cohen MD, Abramson SJ. MR imaging of diffuse bone marrow replacement in pediatric patients with cancer. Radiology. 1991 Nov. 181(2): 587-9.

41. Gosfield E III. AlaviA, Kneeland B. Comparison of radionuclide bone scans and Magnetic Resonance Imaging in detecting spinal metastases. J. Nucl Med. 1993 Dec; 34(12):2191-8.

42. Flickinger FW, Sanal SM. Bone marrow MRI: techniques and accuracy for detecting breast cancer metastases. MagnReson Imaging. 1994; 12(6) : 829-35.

43. Venz S. Hosten N, Friedrichs R, Neumann K, Cordes M, Nagel R, Felix R. Osteoblastic bone metastases in prostatic carcinoma: magnetic resonance tomography and bone marrow scintigraphy. Roof. 1994 Jul; 161(1):64-9.

44. Cesani F, Chaljub G, Briscoe E. Assessment of spinal metastases by bone scintigraphy and magnetic resonace imaging. J Nucl Med. 1995; 36 (suppl): 26.

45. Sauvage PJ, Thivolle P, Noel JB, Dagognet J, Quipourt V, Auberger R. Marchal F, Robert J. MRI in he early diagnosis of spinal metastases of bronchial cancer. J Radiol. 1996 Mar/ 77(3): 185-90.

46. Slovis TL, Meza MP, Cushing B, Elkowitz SS. Leonidas JC, Festa R. Kogutt MS, Fletcher BD. Thoracic neuroblastoma; what is the best imaging modality for evaluating extent of disease? PediatrRadiol. 1997 Mar; 27(3): 273-5.

47. Sardanelli F, Melani E, Sabattini R, Parodi RC, Castaldi A, Rescinito G, Mariani G, Luzzani M. The role of T2*-weighted gradient-echo magnetic resonance sequences in he study of suspected dorsal-lumbosacral vertebral metastases. Radiol Med (Torino). 1997 Oct; 94(4):296-301.

48. Eustace S, Tello R, DeCarvalho V. a comparsion of whole body TurboSTR MR imaging and planar Tc-99m diphosphonatescintugraphy in the examination of patients with suspected skeletal metastases. AJR. 1997; 169:1655-1661.

49. Gibri F, Doppman JL, Reynolds JC, Chen CC, Sutliff VE, Yu F, Serrano J, Venzon DJ, Jensen RT. Bone metastases in patients with gastrinomas: a prospective study of the bone scanning, somatostatin receptor scanning, and magnetic resonance image in their detection, frequency, location and effect of their detection on manageemtn. J ClinOncol. 1998 Mar; 16(3) : 1040-53.

50. Layer G, Steudel A. Schuller H, van Kaick G. Grunwald F, Reiser M, Schild HH. Magnetic resonance imaging to detect bone marrow metastases in the initial staging of small cell lung carcinoma and breast carcinoma. Cancer. 1999 Feb 15; 85(4) 1004-9.

51. Freedman GM, Negendank WG, Hudes GR, Shaer AH, Hanks GE. Preliminary results of a bone marrow magnetic resonance imaging protocol for patients with high-risk prostate cancer. Urology. 1999; 54(1):11823.

52. Saip P, Tenekeci N, Aydiner A, Dincer M, Inanc S, Demir C, Oral EN, Topuz E. Responses evaluation of bone metastases in breast cancer; Value o Magnetic Resonance Imaging. Cancer Invest. 1999; 17(8)"575-80.

53. Greenfield LD,. Bennett LR. Bone scanning. Am Fam Physician. 1975 Mar/ 11(3);84-9.

54. Merrick MV. Review article-Bone scanning. Br J Radiol. 1975 May; 48(569); 327-51.

55. McCready VR. Milestones in Nuclear Medicine. Eur J Nucle Med. 2000; 27 (1 Supply) : S49-79.

56. Ell PJ. Nuclear Medicine. Postgrand Med. J. 1992 Feb; 68(76) : 82-105.

57. Goldstein HA. Bone scintigraphy. OrthopClinNorty Am. 1983 Jan; 14(1):243-56.

58. Malmud LS, Charkes ND. Bone scanning : Principles, Technique and interpretation ClinOrthop. 1975; 107:112-22.

59. Carrington and AD Mclachian, Introduction t magnetic resonance. Chapman and Hall, London, 1967.

60. R Freeman, A Handbook of Nuclear magnetic Resonance, Longman scientific & technical, Essex, England, 1888.

61. Krasnow AZ, Hellman RS. Timins ME. Diagnostic bone scanning in Oncology, SeminNucle Med. 1997 Apr; 27(2) 107-41.

62. Hirano T, Otake H, Kanuma M. Scintigraphic "doughnut sign" on bone scintigraphy secondary o metastatic hepatocellular carcinoma. Clin Med. 1995; 20; 1020. 21.

63. Rybak LD, Rosenthal LD. Radiological imaging for the diagnosis of bone metastases. Q Nucl Med. 2001 Mar; 45(1):53-64.

64. Schwetizer ME, Levine C, Mitchell D, Gannon FH, Gomella LG. Bull's-eys and halos: useful MR discriminator of osseous metastases. Radiology. 1993; 188:249-52.

65. Uchida N, Sugimara K Kajitani A, Yoshizako T, Ishida T. MR imaging of vertebral metastases; evaluation of fat saturation imaging. Eur J Radio. 1993:17:91-4.
66. Boser DI, Todd CEC, Coleman R. Bone secondaries in breast cancer: the solitary metastasis. J Nucl Med. 1989;30:1318-20.
67. Ahmed A. Glynne-Jones R, Ell PJ. Skeletal scintigraphy in carcinoma of the breast: A 10 year retrospective study of 389 patients. Nucl Med Commun. 1990; 11:421-26.
68. Resnick D. skeletal metastatic disease: its articular manifestations. OrthopRav. 1985; (5) : 98-104.
69. Rana A, Chisholm GD, Kahn M, et al. Patterns of bone metastases and their prognostic significance in patients with carcinoma of the prostrate. Br. J Urol. 1993; 72: 933-36.